Electronic Supplementary Material (ESI) for ChemComm.
This journal is © The Royal Society of Chemistry 2014

Supplementary Information

1. Synthesis of sensing molecules

General Procedures: All reactions were carried out under a nitrogen atmosphere using Schlenk techniques, apart from the ester deprotection step. Work up was done in air. Reagent grade methanol, ethyl acetate, dichloromethane, and tetrahydrofuran were used without further purification. Dimethoxyethane (DME) and dimethylformamide (DMF) were distilled from molecular sieves (4 Å). Literature procedures were used to prepare 5-[6-carboxy-indol-2-yl]-5'-methyl-BAPTA ethyl ester **(1),**[1,2] 4-ArmPEG mercaptoacetic acid ester,[3] and BAPTA aldehyde **(8)**,[1] with only a small difference in the first step (substitution reaction) due to other starting compounds. All other chemicals were used as obtained from commercial suppliers. IR spectra were obtained on a Bruker TENSOR 27 instrument. NMR spectra were measured on a Varian INOVA A-400 spectrometer at 400 MHz for ^{1}H and on a Bruker-AVANCE III 500 spectrometer at 500 MHz for ^{1}H, and 125.8 MHz for $^{13}C\{^{1}H\}$. Chemical shifts for ^{1}H and ^{13}C are given in ppm relative to TMS. The UV-vis spectra were recorded on a Varian CARY 50 Scan UV-visible spectrometer. Fluorescence spectra were recorded on a Tekan Infinite® m200 PRO plate reader. LCQMS data were obtained from a LCQ Advantage MAX instrument. The PAAm gels and agarose stamps were prepared using the method reported by Grzybowski *et al.*[4] and Huck *et al.*[5] The overall synthetic route leading to Indo-1 derivatives is presented in Scheme S1, and the one towards a linker-functionalized BAPTA derivative in Scheme S2.

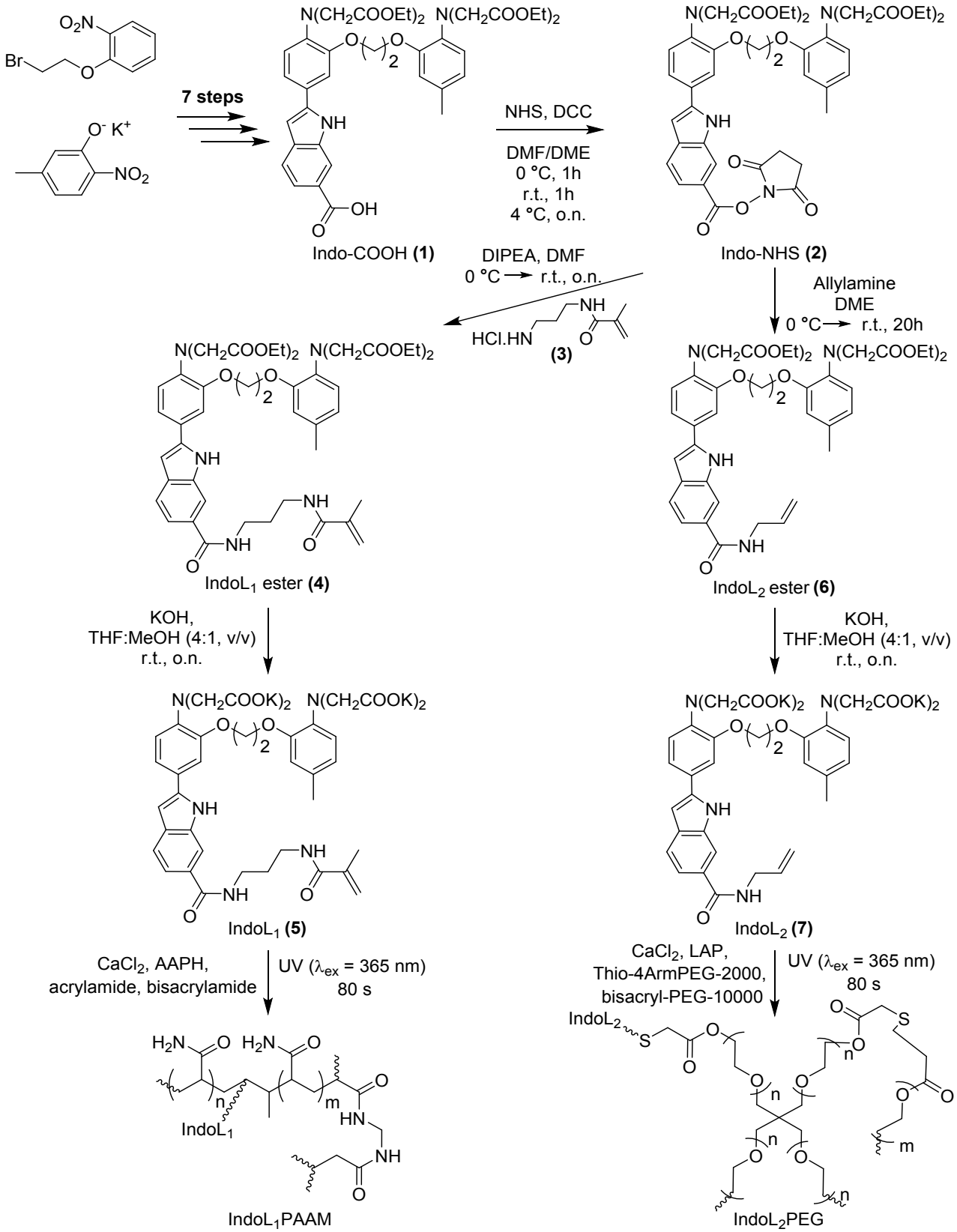

Scheme S1: Synthetic route towards linker-functionalized Indo-1 derivatives, and their

subsequent incorporation into hydrogels.

5-[6-(N-succinimidylcarboxy)indol-2-yl]-5'-methyl-BAPTA ethyl ester (2). Carboxylic acid **(1)** (60 mg, 0.078 mmol) and *N*-hydroxysuccinimide (11 mg, 0.094 mmol) were dissolved in dry dimethylformamide (0.6 mL) under an argon atmosphere. The solution was cooled down to 0 °C, and 1-ethyl-3-(3-dimethylaminopropyl) carbodiimide hydrochloride (EDC·HCl) (18 mg, 0.094 mmol) was added. The reaction mixture was stirred for one hour at 0 °C, and subsequently overnight at room temperature. DMF was removed *in vacuo*. Solid residual was dissolved in ethyl acetate and washed by $KHSO_4$ (10 % , 2 x 2 mL) and water (2 x 2 mL). The solution was dried over Na_2SO_4 and concentrated. The residue was purified by column chromatography (SiO_2, Toluene/EtOAc 2:1, Rf ~ 0.3). Yield: 46 mg (0.0546 mmol, 70 %). IR (cm^{-1}): 3356 (NH), 1734 (CO). NMR: ^{1}H (500 MHz, $CDCl_3$) δ = 9.83 (s, 1H, N*H*), 8.13 (s, 1H, Ar), 7.67 (dd, $J_{H\text{-}H}$ = 8.4 Hz, $J_{H\text{-}H}$ = 1.5 Hz, 1H, Ar), 7.48 (d, $J_{H\text{-}H}$ = 8.4 Hz, 1H, Ar), 7.32 (m, 2H, Ar), 6.85 (d, $J_{H\text{-}H}$ = 8.3 Hz, 1H, Ar), 6.76 (d, $J_{H\text{-}H}$ = 7.9 Hz, 1H, Ar), 6.69 (m, 3H, Ar), 4.38 (m, 2H, OCH_2CH_2O), 4.25 (m, 2H, OCH_2CH_2O), 4.19 (s, 4H, NCH_2CO), 4.15 (s, 4H, NCH_2CO), 4.10 (m, 8H, CH_2CH_3), 2.92 (s, 4H, NHS), 2.25 (s, 3H, CH_3) 1.21 (t, $^2J_{H\text{-}H}$ = 7.1 Hz, 6H, CH_2CH_3), 1.16 (t, $^2J_{H\text{-}H}$ = 7.1 Hz, 6H, CH_2CH_3). ^{13}C (125 MHz, $CDCl_3$) δ = 171.91, 171.33, 170.13, 162.90, 150.24, 150.23, 142.77, 140.26, 136.83, 135.80, 134.46, 132.27, 125.24, 121.99, 121.52, 119.89, 119.79, 119.29, 119.01, 116.56, 114.60, 114.45, 112.20, 99.10, 68.06, 67.16, 60.96, 60.94, 53.80, 53.68, 25.81, 20.92, 14.13, 14.08. MS (ESI): *m*/*z* 857.1 (M^- [$C_{39}H_{44}N_5O_9$] = 857.3)

5-[6-(N-(3-methacrylamidopropyl)carboxyamide)indol-2-yl]-5'-methyl-BAPTA ethyl ester (4) A solution of *N*-(3-aminopropyl)methacrylamide hydrochloride **(3)** (11 mg, 64 μmol) in 0.5 mL of dimethylformamide (DMF) was added to the mixture of Indo-NHS ester **(2)** (46 mg, 53.6 μmol) and diisopropylethylamine (10 mg, 80 μmol) in DMF (0.5 mL) at 0 °C. The reaction mixture was allowed to come to room temperature, and was stirred o.n. Then, the solvent was evaporated, and column chromatography eluting with ethyl acetate – toluene (10:1) yielded the desired IndoL_1 ester **(4)** (24 mg, 27.1 μmol, 50%). IR (cm^{-1}): 3350 (NH), 1714 (CO). ^{1}H NMR (400 MHz, $CDCl_3$) δ 9.65 (s, 1H, N*H*), 8.00 (s, 1H, Ar), 7.61 – 7.50 (m, 2H, Ar), 7.28 (m, 1H, Ar), 7.11 – 6.63 (m, 6H, Ar), 5.81 (s, 1H, CCH_2), 5.34 (s, 1H, CCH_2), 4.33 (s, 1H, OCH_2CH_2O), 4.23 – 4.05 (m, 19H, OCH_2CH_2O, OCH_2CH_2O, NCH_2CO, OCH_2CH_3), 3.52 (dd, $^2J_{H\text{-}H}$ = 12.1 Hz, $^2J_{H\text{-}H}$ = 6.2 Hz, 2H, CH_2CH_2CH_2), 3.42 (dd, $^2J_{H\text{-}H}$ = 12.1 Hz, $^2J_{H\text{-}H}$ = 6.3 Hz, 2H,

$CH_2CH_2CH_2$), 2.24 (s, 3H, $ArCH_3$), 2.00 (s, 3H, CCH_3), 1.83 – 1.72 (m, 2H, $CH_2CH_2CH_2$), 1.28 – 1.13 (m, 12H, CH_2CH_3) ^{13}C NMR (125 MHz, $CDCl_3$) δ 172.31, 171.89, 171.43, 169.41, 169.24, 150.31, 150.23, 140.97, 139.70, 139.43, 136.69, 136.51, 132.30, 131.92, 127.03, 125.97, 121.84, 120.12, 119.79, 119.14, 118.85, 118.40, 114.33, 111.27, 110.87, 98.42, 77.61, 77.29, 77.04, 76.79, 67.63, 66.99, 60.94, 60.91, 53.78, 53.72, 36.43, 36.16, 29.77, 25.30, 20.92, 18.66, 14.08, 14.04. MS (ESI): *m*/*z* 885.4 (M^+ [$C_{47}H_{59}N_5O_{12}$] = 886.2, $(M+Na)^+$ = 908.4)

5-[6-(N-(3-methacrylamidopropyl)carboxyamide)indol-2-yl]-5'-methyl-BAPTA potassium salt (5) $IndoL_1$ ester **(4)** (19.5 mg, 21.0 µmol) was dissolved in 1056 µL THF – MeOH (4:1, v/v), and 121 µL KOH (1 M) was added. The light yellow reaction mixture was stirred overnight at room temperature in the dark, after which the colour had changed to light brown. After the addition of THF (approx. 0.5 mL) and stirring for five minutes, white clouds of precipitation were observed, and the colour of the solution had become deep purple. The crude reaction mixture was transferred to an Eppendorf tube, and centrifuged (12,000 rpm, 30 s, r.t.). Then, the supernatant was removed and the residue washed twice with THF. After another round of centrifugation and removal of the supernatant, the residue was dried to yield the desired $IndoL_1$ **(5)** (14.5 mg, 15.7 µmol, 74%) as a white powder. IR (cm^{-1}): 3274 (NH). ^1H NMR (400 MHz, D_2O) δ 7.93 (s, 1H, Ar), 7.71 (d, J_{H-H} = 8.4 Hz, 1H, Ar), 7.49 (dd, $^2J_{H-H}$ = 8.4 Hz, $^2J_{H-H}$ = 1.6 Hz, 1H, Ar), 7.45 (d, J_{H-H} = 1.9 Hz, 1H, Ar), 7.41 (dd, $^2J_{H-H}$ = 8.4 Hz, $^2J_{H-H}$ = 2.0 Hz, 1H, Ar), 6.93 (s, 1H, Ar), 6.89 (d, J_{H-H} = 0.6 Hz, 1H, Ar), 6.86 (d, J_{H-H} = 8.5 Hz, 1H, Ar), 6.79 (s, 2H, Ar), 5.69– 5.67 (m, 1H, CCH_2), 5.43 – 5.40 (m, 1H, CCH_2), 4.30 (dd, ^2J = 16.3 Hz, $^2J_{H-H}$ = 4.7 Hz, 4H, OCH_2CH_2O), 3.89 (s, 4H, NCH_2CO), 3.79 (s, 4H, NCH_2CO), 3.47 (t, J_{H-H} = 6.7 Hz, 2H, $CH_2CH_2CH_2$), 3.37 (t, J_{H-H} = 6.6 Hz, 2H, $CH_2CH_2CH_2$), 2.26 (s, 3H, $ArCH_3$), 1.94 – 1.83 (m, 5H, CCH_3, $CH_2CH_2CH_2$). ^{13}C NMR (126 MHz, MeOD) δ 180.08, 177.01, 176.73, 170.29, 169.96, 150.77, 150.44, 141.22, 140.59, 139.92, 137.93, 136.73, 132.51, 132.07, 126.78, 120.93, 119.20, 119.12, 118.23, 118.09, 117.89, 117.73, 112.09, 110.43, 108.43, 97.97, 67.45, 66.24, 65.82, 57.86, 57.73, 36.84, 36.58, 34.66, 34.27, 30.23, 29.15, 25.09, 19.79, 17.41. MS (ESI): *m*/*z* 773.3 (M^- [$C_{39}H_{43}N_5O_{12}$] = 772.5)

5-[6-(N-(allyl)carboxyamide)indol-2-yl]-5'-methyl-BAPTA ethyl ester (6) Allylamine (2 mg, 46 µmol) was added to a solution of NHS ester **(2)** (25 mg, 28 µmol) in anhydrous dimethoxyethane (DME) (0.5 mL) at 0 ºC. The mixture was stirred at r.t. for 20 h and filtered.

The precipitate was collected and washed by methanol to give pure product. Yield: 9 mg (12 µmol, 43 %). IR (cm^{-1}): 3356 (NH), 1734 (CO). ^{1}H NMR (500 MHz, $CDCl_3$) δ 9.61 (s, 1H, N*H*), 8.03 (s, 1H, Ar), 7.60 (d, $J_{H\text{-}H}$ = 8.3 Hz, 1H, Ar), 7.46 (d, $J_{H\text{-}H}$ = 8.3 Hz, 1H, Ar), 7.30 (m, 2H, Ar), 6.87 (d, $J_{H\text{-}H}$ = 8.2 Hz, 1H, Ar), 6.79 (d, $^2J_{H\text{-}H}$ = 8.0 Hz, 1H, Ar), 6.71 (m, 3H, Ar), 6.37 (s, 1H, Ar), 6.00 (ddd, $^2J_{H\text{-}H}$ = 22.4, $^2J_{H\text{-}H}$ = 10.7, $^2J_{H\text{-}H}$ = 5.6 Hz, 1H, C*H*=CH_2), 5.31 (d, $^2J_{H\text{-}H}$ = 17.5 Hz, 1H, CH=C*H*$_2$), 5.20 (d, $^2J_{H\text{-}H}$ = 10.2 Hz, 1H, CH=C*H*$_2$), 4.35 (m, 2H, OCH_2CH_2O), 4.25 – 4.07 (m, 18H, OCH_2CH_2O, NCH_2CO, CH_2CH_3), 2.27 (s, 3H, C*H*$_3$), 1.24 (t, $J_{H\text{-}H}$ = 7.1 Hz, 6H, CH_2CH_3), 1.19 (t, $J_{H\text{-}H}$ = 7.1 Hz, 6H, CH_2CH_3). ^{13}C NMR (125 MHz, $CDCl_3$) δ = 171.92, 171.34, 168.24, 150.31, 150.28, 140.80, 139.80, 136.87, 136.53, 134.61, 132.30, 131.87, 127.43, 125.90, 122.00, 119.75, 119.42, 119.33, 119.01, 117.94, 116.36, 114.77, 112.22, 111.14, 98.57, 77.58, 68.03, 67.19, 60.91, 53.85, 53.74, 42.50, 20.92, 14.14, 14.10.

5-[6-(N-(allyl)carboxyamide)indol-2-yl]-5'-methyl-BAPTA potassium salt (7) $IndoL_2$ ester **(6)** (9 mg, 12 µmol) was dissolved in tetrahydrofuran – methanol (4:1, v/v, 750 µL), and 86 µL KOH (1 M) was added. The reaction mixture was stirred overnight at room temperature, after which the colour had changed from reddish to deep purple. By adding tetrahydrofuran, precipitation of the product was initiated and in the still purple mixture white clouds of precipitate were observed. The crude reaction mixture was filtered, and the residue dried to yield the desired tetracarboxylic acid **6** (6 mg, 7 µmol, 58%).) IR (cm^{-1}): 3317 (NH), 1574 (CO). ^{1}H NMR (500 MHz, MeOD) δ = 7.97 (s, 1H, Ar), 7.60 (s, 1H, Ar), 7.58 (s, 1H, Ar), 7.55 – 7.48 (m, 2H, Ar), 7.41 (dd, $J_{H\text{-}H}$ = 8.2, $^2J_{H\text{-}H}$ = 1.8 Hz, 1H, Ar), 7.11 (d, $^2J_{H\text{-}H}$ = 8.3 Hz, 1H, Ar), 6.94 (d, $^2J_{H\text{-}H}$ = 8.0 Hz, 1H, Ar), 6.88 (s, 1H, Ar), 6.85 (s, 1H, Ar), 6.73 (d, $^2J_{H\text{-}H}$ = 7.4 Hz, 1H, Ar), 6.00 (ddt, $^2J_{H\text{-}H}$ = 17.1, $^2J_{H\text{-}H}$ = 10.5, $^2J_{H\text{-}H}$ = 5.4 Hz, 1H, C*H*=CH_2), 5.29 (dd, $^2J_{H\text{-}H}$ = 17.2, $^2J_{H\text{-}H}$ = 1.6 Hz, 1H), 5.17 (dd, $^2J_{H\text{-}H}$ = 10.3, $^2J_{H\text{-}H}$ = 1.5 Hz, 1H), 4.54 (s, 2H, OCH_2CH_2O), 4.45 (s, 2H, OCH_2CH_2O), 4.06 (d, $^2J_{H\text{-}H}$ = 5.4 Hz, 2H, NH-C*H*$_2$), 3.63 (s, 4H, NCH_2CO), 3.55 (s, 4H, NCH_2CO), 2.33 (s, 3H, C*H*$_3$).^{13}C NMR (126 MHz, MeOD) δ 177.01, 176.74, 170.00, 150.78, 150.46, 141.23, 140.62, 137.95, 136.71, 134.57, 132.47, 132.08, 126.76, 120.90, 119.16, 118.18, 118.08, 117.92, 117.69, 114.57, 112.08, 110.47, 108.45, 97.94, 66.24, 65.80, 57.87, 57.72, 48.44, 41.94, 19.77. MS (ESI): *m*/*z* 687.4 (M^- [$C_{35}H_{36}N_4O_{11}$] = 687.2)

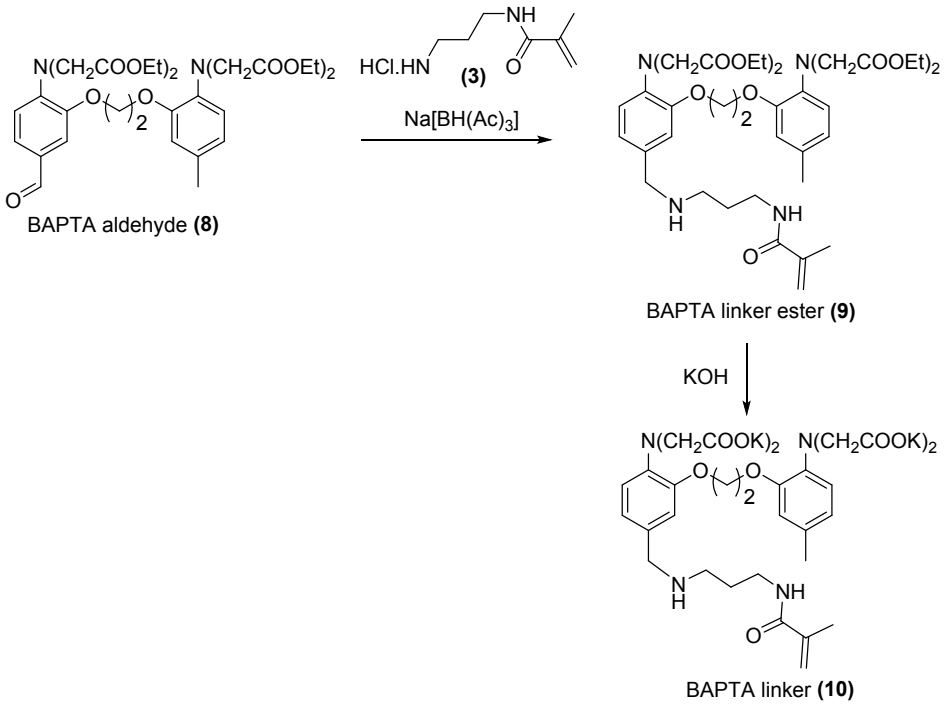

Scheme S2: Synthesis of the BAPTA derivative with acrylamide linker.

5-[((3-methacrylamidopropyl)amino)methyl]-5'-methyl-BAPTA ethyl ester (purity about 80%) (9). 5-Formyl-5'-methyl-BAPTA ethyl ester **(8)** (400 mg, 0.63 mmol) was added to a mixture of *N*-(3-aminopropyl)methacrylamide (140 mg, 0.756 mmol) and triethylamine (70 mg, 0.69 mmol) in THF. The solution was stirred for 15 min. Some precipitate could be present at this stage. Sodium triacetoxyborohydride (204 mg, 0.95 mmol) was added and the mixture was stirred for 2 hours a r.t. under a nitrogen atmosphere. The reaction was then quenched with 5 mL of 5 % solution of $NaHCO_3$ and extracted with ethyl acetate (3 x 5 mL). The organic phase was washed with $NaHCO_3$ (5 %, 2 x 5 mL) and water (2 x 5 mL). The solution was dried over Na_2SO_4 and concentrated to give (270 mg) of crude product. It was only 80-85% pure according to ^{1}H NMR, but attempts to purify the product by column chromatography or by precipitation as a salt were unsuccessful. We decided to proceed with the crude product expecting that the compound would be suitable for making BAPTA-modified PAAm hydrogels. ^{1}H NMR (400 MHz, $CDCl_3$) δ = 6.85 – 6.60 (m, 7H), 5.67 (m, 1H), 5.7 (m, 1H), 4.27 (s, 4H), 4.14 (s, 4H), 4.12 (s, 4H), 4.10 – 4.00 (m, 8H), 3.68 (s, 4H), 3.42 (dd, J = 12.0, 5.7 Hz, 2H), 2.74 (t, J = 6.0 Hz, 2H), 2.26 (s, 1H), 1.92 (d, J = 0.6 Hz, 2H), 1.70 (dt, J = 12.2, 6.1 Hz, 2H), 1.16 (t, J = 7.1, 12H).

5-[((3-methacrylamidopropyl)amino)methyl]-5'-methyl-BAPTA potassium salt (purity about 80%) (10).

Ester **(9)** (170 mg, 225 μmol) was dissolved in tetrahydrofuran – methanol (8:1, v/v, 9 mL), and 1.3 mL of KOH water solution (1 M) were added. The reaction mixture was stirred overnight at room temperature. Then, the solvent was evaporated to dryness, and the residue was dissolved in 0.5 mL of isopropanol. Addition of tetrahydrofuran induced precipitation of the product. The crude product was filtered and dried. Yield (150 mg, 189 μmol, 58%). The product was used for copolymerization without further purification. ^{1}H NMR (400 MHz, D_2O) δ 6.92 – 6.53 (m, 8H), 5.47 – 5.40 (m, 1H), 5.24 (dd, *J* = 1.5, 1.1 Hz, 1H), 4.19 (s, 4H), 3.60 – 3.53 (s, 8H, m), 3.49 (s, 2H), 3.09 (t, *J* = 6.7 Hz, 2H), 2.43 – 2.36 (m, 2H), 2.09 (s, 3H), 1.71 (s, 3H), 1.54 (dt, *J* = 14.1, 6.9 Hz, 2H).

2. Preparation of Ca^{2+}-binding and –responsive hydrogels

Preparation of BAPTA-functionalized gel for Ca^{2+} complexation.

Acrylamide (485 mg), bisacrylamide (20 mg), and potassium salt **10** (20 mg) were dissolved in 5 mL MilliQ. An aliquot of 2 mL was then taken and deoxygenated by argon. Subsequently, the solution was mixed with AAPH (20 μL, 150 mg/ml) and poured onto a hydrophobic glass slide, and covered with another slide, which rested on two small other parts with a thickness of 1 mm. The gel was formed by irradiating the solution with UV (365 nm) for 2 minutes. The gel was washed four times by 30 mM MOPS, 100 mM KCl buffer pH 7.20. The gel was then used to prepare Ca^{2+}- and Ca^{2+}-chelator free buffers.

Polyacrylamide hydrogel

Acrylamide (485 mg) and bisacrylamide (20 mg) were dissolved in 5 mL MilliQ. An aliquot of 2 mL was then taken, and $IndoL_1$ **(5)** was added (20 μL of 1 mM in D_2O) to create solution 1. A few microliters of highly concentrated $CaCl_2$ in MilliQ were added to fully saturate the indicator. Solution 2 was prepared by dissolving 150 mg of 2,2'-azobis-2-methylpropanimidamide dihydrochloride (AAPH) in 1 mL of MilliQ. Next, 20 μL of solution 2 was added to solution 1. The resulting solution 3 was then deoxygenated by bubbling with argon for 30 seconds. Subsequently, solution 3 was poured onto a hydrophobic glass slide, and covered with another

slide, which rested on two small other parts with a thickness of 0.4 mm. At this point, it was crucial that solution 3 overflowed the glass slides, since gels with inhomogeneous fluorescence at the edges would be formed otherwise. Polymerization was initiated by irradiating with UV (365 nm) for 80 seconds at 4 cm from the UV lamp. Then, the lamp was switched off and the $IndoL_1PAAm$ gel was allowed to maximally polymerize by letting it rest for a few minutes without perturbation. The gel was then washed with a BAPTA-containing buffer to remove the excess of Ca^{2+} used during polymerization. Next, the hydrogel was treated with a BAPTA-free buffer to remove the Ca^{2+}-chelating species. Finally, the hydrogel was placed in buffer (30 mM MOPS, 100 mM KCl, pH 7.20) together with a BAPTA-functionalized gel (see previous page) to remove residual amounts of Ca^{2+}, and to ensure that no BAPTA would be present in the $IndoL_1PAAm$ gel.

Polyethylene glycol hydrogel

4-ArmPEG (Mw 2000, see Fig. S1) mercaptoacetic acid ester (10 mg), PEG acrylate (Mw 10000) (81 mg) and LAP (1.5 mg) were dissolve d in 965 µL MilliQ. Then, $IndoL_2$ (25 µL, 1 mg/ml) and $CaCl_2$ (5 µL, 100 mM) were added. The resulting solution was purged with argon for 30 seconds to remove oxygen. Subsequently, the solution was poured onto a hydrophobic glass slide, covered with another slide, and irradiated with UV (365 nm) for 2 minutes. At this point, it was crucial that solution 3 overflowed the glass slides, since gels with inhomogeneous fluorescence at the edges would be formed otherwise. Polymerization was initiated by irradiating with UV (365 nm) for 80 seconds at 4 cm from the UV lamp. The gel was then washed with a BAPTA-containing buffer, and a BAPTA-free buffer before use in experiments. The gel swelled to about 400 % its initial size during washing.

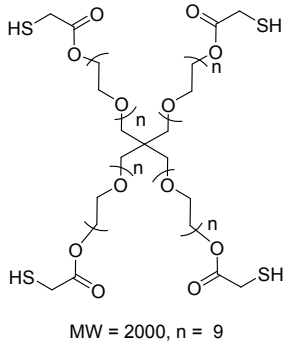

Figure S1: Structure of Thio-4ArmPEG-2000.

3. Determination of dissociation constants using Ca^{2+} titration

$IndoL_1$ and $IndoL_2$ in solution

We measured the K_D of compounds $IndoL_1$ and $IndoL_2$ in solution using the Calcium Calibration Buffer Kit purchased from Invitrogen. We prepared 11 solutions with different concentrations of Ca^{2+} as shown in Table S1, using zero free Ca^{2+} solution (10 mM EGTA, 30 mM MOPS, 100 mM KCl, pH 7.2) and 39 µM free Ca^{2+} solution (10 mM CaEGTA, 30 mM MOPS, 100 mM KCl, pH 7.2). These solutions were placed in a 96 well plate, mixed with stock solutions of $IndoL_1$ and $IndoL_2$ to obtain a final concentration of 1 µM of the indicator. Spectra were obtained with a Tekan Infinite® m200 PRO plate reader at 20 ^oC with excitation wavelengths of 360 and 350 nm for $IndoL_1$ and $IndoL_2$, respectively. K_D's for both compounds were calculated as described in the manual provided by Invitrogen. The K_D of $IndoL_1$ was found to be 514 nM, and for $IndoL_2$ this constant was 340 nM.

Table S1: Different mixtures of zero free Ca^{2+} solution and 39 µM free Ca^{2+} solution used in the titration experiment to obtain different final concentrations of free Ca^{2+}.

[CaEGTA] (in mM)	$[Ca^{2+}]_{free}$ (in µM)	Volume of zero free Ca^{2+} solution added (in µL)	Volume of 39 µM free Ca^{2+} solution added (in µL)
0	0	200	0
1	0.017	180	20
2	0.038	160	40
3	0.065	140	60
4	0.1	120	80
5	0.15	100	100
6	0.225	80	120
7	0.351	60	140
8	0.602	40	160
9	1.35	20	180
10	39	0	200

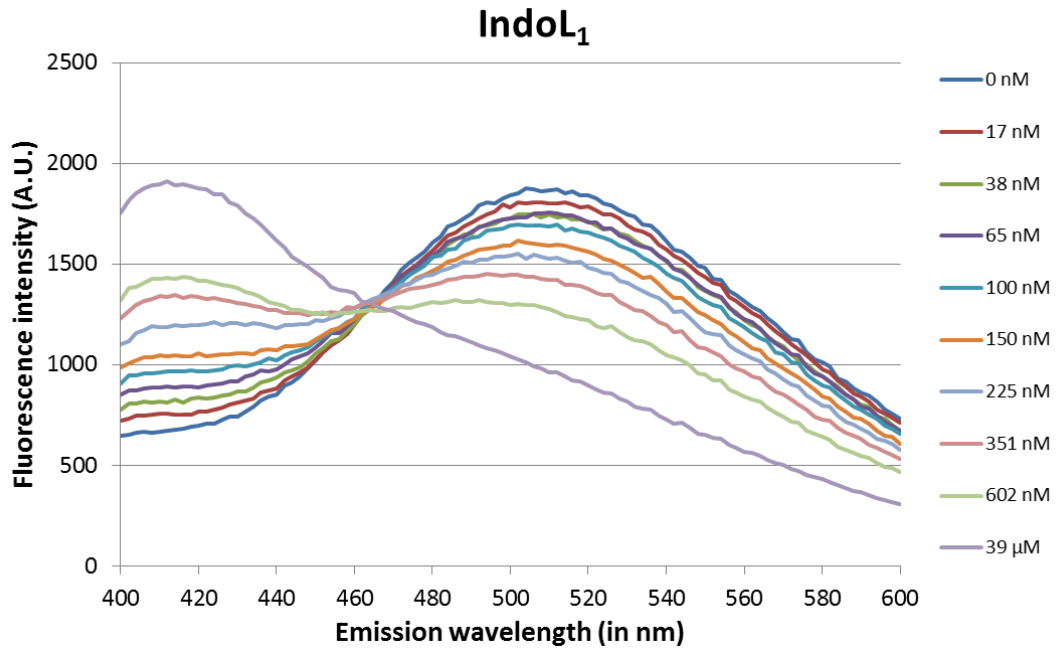

Figure S2: Calibration of $IndoL_1$ with different concentrations of Ca^{2+}.

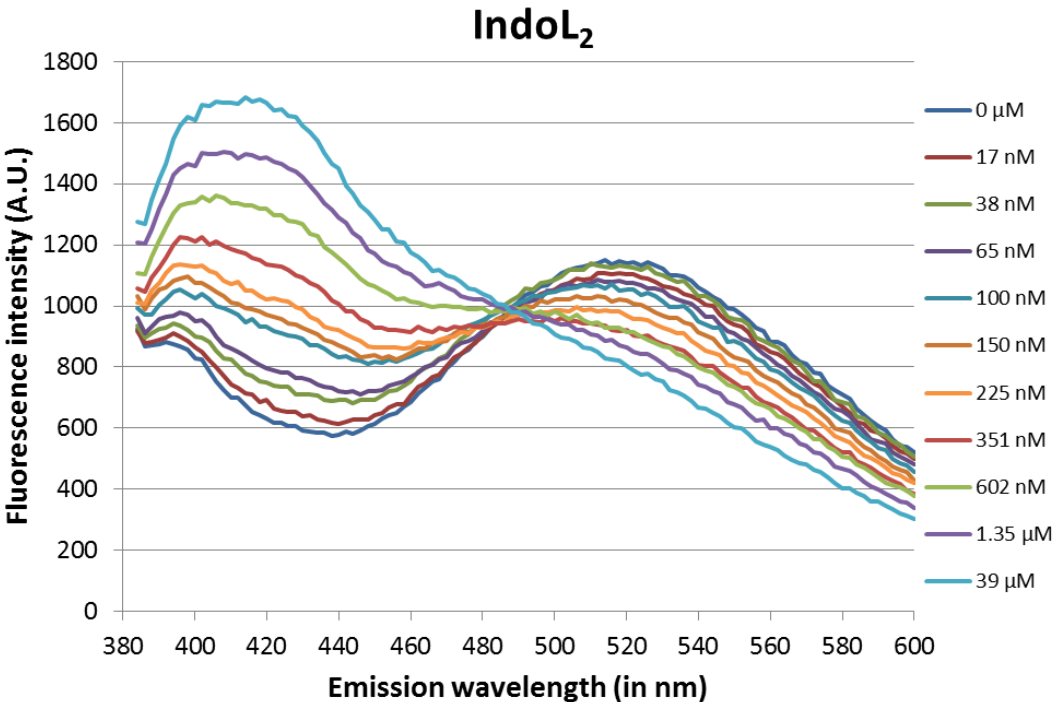

Figure S3: Calibration of $IndoL_2$ with different concentrations of Ca^{2+}.

4. Selectivity of IndoL$_1$ towards Ca^{2+}

To show the selectivity of IndoL$_1$ towards Ca^{2+}, we measured spectra of 1 µM of indicator in presence of varying concentrations of Mg^{2+}. The resulting data in Fig. S4 show hardly any change in spectra at range of Mg^{2+} concentrations from 0.2 to 1 mM.

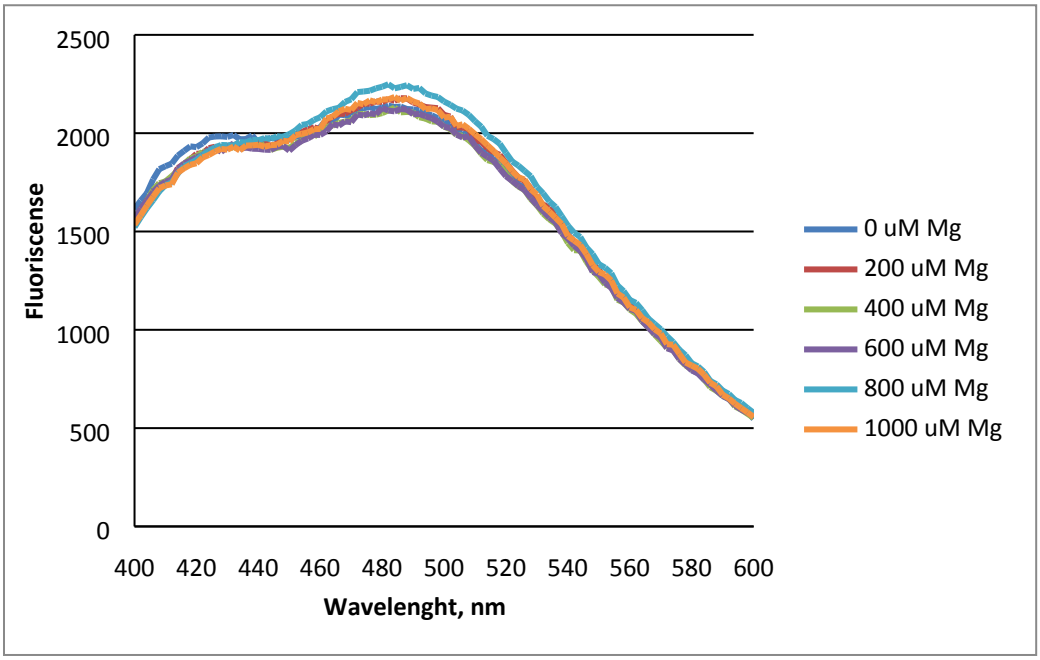

Figure S4 Spectra of IndoL$_1$ in presence of Mg^{2+}.

5. Reversibility of gel response

To show that the PAAmIndoL$_1$ gel can reversibly detect Ca^{2+} we soaked a piece of gel first in a 50 µM solution of $CaCl_2$ in MOPS buffer at pH 7.2. Next, the gel was washed in MOPS buffer without added EGTA or Ca^{2+}. Then, the gel was placed in a 50 µM solution of EGTA in MOPS buffer pH 7.2. This cycle was repeated several times, as is depicted in Figure S5. After each soaking step, the gel was imaged with fluorescence microscopy, and the ratio of fluorescence intensities at 520 and 405 nm emission wavelength was measured as described in the main text. Thus, it was shown that PAAmIndoL$_1$ indeed detects Ca^{2+} in a reversible manner, which is of importance for *e.g.* future studies on pattern formation.

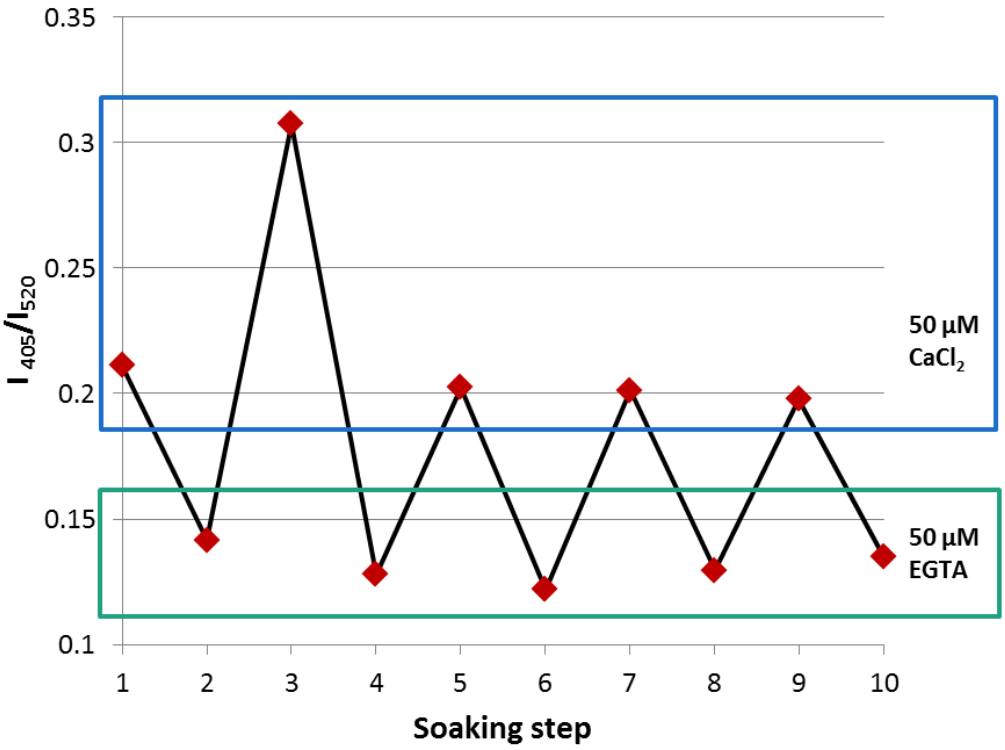

Figure S5: Reversibility of Ca^{2+}-binding by the PAAmIndoL$_1$ hydrogel.

6. Fluorescence Recovery After Photobleaching (FRAP) experiment

For the FRAP experiment, two PAAm gels were prepared. For sample 1 (see Figure 1Ai in the main text) the gel was prepared as described in paragraph 2 of this ESI, but in the absence of IndoL$_1$. After washing with buffer, the gel was placed in a solution of 10 µM IndoL$_1$. The second PAAm gel (see Figure 1Aii in the main text) was prepared in the presence of 10 µM IndoL$_1$, as described in paragraph 2 of this ESI, so that the indicator was copolymerized. Subsequently, a circular area was bleached in each gel by irradiation with a 20x objective for approximately 20 seconds. Thereafter, images were taken with a 2x objective each 5 minutes for sample 1. After 10 minutes, the fluorescence was almost fully restored in the bleached region due to diffusion of the indicator.

For sample 2, images were also recorded several minutes after bleaching, but no change was visible. Then, a plastic cap with moist paper on the inside was placed over the gel (without touching it) to prevent the PAAmIndoL$_1$ hydrogel from drying out. Two days later, another image was taken, and no change in the photobleached area was observed. Therefore, it was concluded that the indicator was covalently linked to the PAAm gel. Furthermore, it was shown

that diffusion of the indicator (in sample 1) occurred on the same timescale as Ca^{2+} diffusion (see Figure 3 of main text), underpinning the importance of immobilizing the indicator for accurate probing of the Ca^{2+} diffusion front.

7. Stamping experiments

For the diffusion experiments, 6 wt% agarose stamps were prepared, and soaked overnight in a Ca^{2+} solution. The volumes of the agarose stamps themselves were taken into account when the final concentration of Ca^{2+} was calculated. PAAmIndoL$_1$ gels were prepared as described in paragraph 2 of this Supplementary Information. A small piece of Ca^{2+}- and BAPTA-free PAAmIndoL$_1$ gel was cut and placed in a Petri dish. Under the UV lamp (λ_{ex} = 365 nm) the gel was predominantly green, but blue at the edges where the gel was touched by the scalpel or tweezers during cutting and transferring the gel. The blue colour did not spread through the gel, indicating that only a small amount of Ca^{2+} was present.

Before the agarose stamp was placed on top of the PAAmIndoL$_1$ gel, it was dried for approximately half a minute on a Kimtech tissue paper. After carefully putting the agarose stamp on top of the PAAmIndoL$_1$ gel, images were taken with the fluorescence microscope (λ_{ex} = 360 nm). After taking an image with a filter for an emission wavelength of 405 nm, the filter was immediately automatically changed to one for an emission wavelength of 520 nm. In this way, the ratio of fluorescence intensities at 405 and 520 nm emission was obtained for each time point during diffusion of Ca^{2+}. A typical diffusion experiment took between 10 and 20 minutes, and significant drying of the gels was not observed during this time period.

8. Image processing

The basic procedure of data analysis consists of the following steps: a) calculation of images with maximum and minimum ratio of I_{405}/I_{520}, b) calculation of I_{405}/I_{520} profiles for each time point c) calculation of Ca^{2+} concentration. Profiles could be assembled into a time-space plot for presentation purposes. Details for each individual step are described below.

Calculation of images with maximum and minimum ratio of I_{405}/I_{520}

To determine the minimum ratio of I_{405}/I_{520}, images of Ca^{2+}-free gel were taken before the experiment. Subsequently, images of Ca^{2+}-saturated gel were taken at the end of an experiment

to determine the maximum ratio of I_{405}/I_{520}. Analysis was performed in the computer program **imageJ**. A ratio of image with emission at 405 nm to image with emission at 520 nm was calculated for each pair of images. A ratiometric image was reconstructed in each case.

Calculation of I_{405}/I_{520} profiles for each time point

Ratiometric images for every time point were reconstructed as described in the previous chapter. Then, for each image (including images with maximum and minimum ratio of I_{405}/I_{520}) a rectangular area (~2000 μm in X direction and ~200 μm in Y direction) was selected. A profile along the X-coordinate was calculated by averaging the intensity in the Y direction. Macro *"CalculateProfiles_fromListOfTiffs.ijm"* was used to calculate list of profiles and macro *"makeKymograph_fromListOfTiffs"* was used to build kymographs (time-space plots), see *"diffusion_analysis.ijm"*.

Calculation of Ca^{2+} concentration

Values of $(R - R_{min})/(R_{max} - R)$, where $R = I_{405}/I_{520}$, were calculated for profiles at each time point. Then, the Ca^{2+} concentration was calculated using a calibration curve (see Fig. 1c of main text). It should be noticed, that this step is applicable only in the approximation of flat reaction-diffusion front (concentrations are equal in Z direction).

ImageJ macro "*diffusion_analysis.ijm*" to create time-space plots

```
macro "makeKymograph_fromListOfTiffs"{
	//input: text file containing full path to each image
	list = openTiffsFromTextFile();
	process(list);
}
macro "getDataForBacgroundCorrection"{
	//input: text file containing full path to each image
	list = openTiffsFromTextFile();
	bacgrCorGetAvAndBgInt(list);
}
function openTiffsFromTextFile(){
	path = File.openDialog("Choose stack file");
	content = File.openAsString(path);
	return split(content, "\n");
}
function process(list) {
// Start of Processing parameters
	anAngle		= 2.82;		//angle to rotate each image
```

```
	x0		= 298;		//rectangle region of interest
	y0		= 534;
	dx		= 554;
	dy		= 106;

	dl		= 11.28;	//spatial calibration: distance per pixel (um/pix)

	bc_Slope = 0.4689964888;
	bc_Intercept = 95.8471499145;
// End of Processing parameters

	dir = File.getParent(list[0]);

	if (getVersion>="1.40e")
		setOption("display labels", true);


	setBatchMode(true);

	kymographID = 0;
	for (i=0; i<list.length; i++) {
		path = list[i];
		showProgress(i, list.length);

		// create kymograph image
		if (i == 0) {
			kymographID = createKymographImage(path, dx, list.length);
			showMessage("imageID for kymograph: " + toString(kymographID));
		}

		if (!endsWith(path,"/")) open(path);
		if (nImages>=1) {
			experimentalImageID = getImageID();

			//rotate image
			run("Rotate... ", "angle=" + toString(anAngle) + " grid=1
interpolation=Bilinear");

			//get average pixel intensity for background correction
			getStatistics(area, tot);

			//pick region of interest and get profile
			makeRectangle(x0, y0, dx, dy);
			profile = getProfile();
```

```
                        //add profile to kymograph image
                        for (n = 0; n < profile.length; n++) {
                                anIntensity = profile[n] - bc_Intercept - bc_Slope * tot;

                                selectImage(kymographID);
                                setPixel(n, i, anIntensity);
                        }

                        selectImage(experimentalImageID);
                        close();

                }
                updateDisplay();
        }
        saveAs("Tiff", dir + "\\kymograph.tif");
        setBatchMode(false);
}
function createKymographImage(title, width, height){
        newImage("kymograph_" + title, "32-bit White", width, height, 1);
        return getImageID();
}
function bacgrCorGetAvAndBgInt(list){
// ROI where background data is obtained
        x0 = 490;
        y0 = 357;
        dx = 36;
        dy = 129;
//////////////////////////////////////////

        dir = File.getParent(list[0]);

        if (getVersion>="1.40e")
                setOption("display labels", true);

        setBatchMode(true);
        run("Clear Results");

        for (i=0; i<list.length; i++) {
                path = list[i];
                showProgress(i, list.length);
                if (!endsWith(path,"/")) open(path);
                if (nImages>=1) {
                        //get average pixel intensity for background correction
                        getStatistics(area, iav);
                        makeRectangle(x0, y0, dx, dy);
                        getStatistics(area, ibgnd);
```

```
                    setResult("Iavg", i, iav);
                    setResult("Ibg", i, ibgnd);
                }
                close();
        }
        updateResults();
        saveAs("Measurements",  dir + "\\bacground.cor.data.txt");
        setBatchMode(false);
}
```

9. Modeling of the RD experiment in COMSOL

In order to get more information from our experiments we simulated the RD experiment with CalB in COMSOL. The model consists of three rectangles (see Fig. S6): the bottom one represents the PAAm gel and the two top ones the agarose stamp.

To model reaction-diffusion of Ca^{2+} we used the reactions and parameters shown in Table S2. The concentration of Ca^{2+} in the agarose stamp was set to 25 µM, the concentration of CalB in the PAAm stamp to 30 µM, and concentration of covalently bound indicator in PAAm gel to 10 µM.

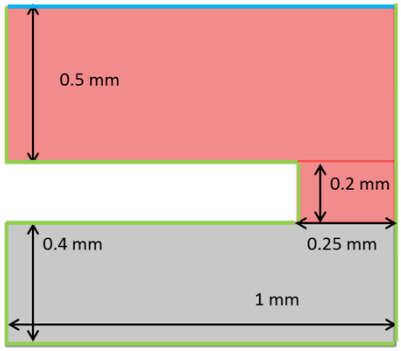

Figure S6: Geometry of our model describing the RD experiment. Red represents agarose and grey PAAm. Over the borders shown as green lines there is no transport of species. At the upper blue border there is a constant concentration of

Table S2: Reactions and constants used in modeling. Reaction rates and diffusion constants were estimated using literature values. [6–8]

Reaction	Rate constants
$Ca + IndoL_1 \Leftrightarrow CaIndo\ L_1$	$k_{on} = 500000\ m^3/(s\cdot mol)$, $k_{off} = 240\ s^{-1}$
$Ca + CalB \Leftrightarrow CaCalB$	$k_{on} = 12000\ m^3/(s\cdot mol)$, $k_{off} = 1.6\ s^{-1}$
$Ca + CaCalB \Leftrightarrow Ca_2CalB$	$k_{on} = 12000\ m^3/(s\cdot mol)$, $k_{off} = 4\ s^{-1}$
$Ca + Ca_2CalB \Leftrightarrow Ca_3CalB$	$k_{on} = 12000\ m^3/(s\cdot mol)$, $k_{off} = 7.2\ s^{-1}$
$Ca + Ca_3CalB \Leftrightarrow Ca_4CalB$	$k_{on} = 12000\ m^3/(s\cdot mol)$, $k_{off} = 14\ s^{-1}$
Diffusion of Ca^{2+}	$D_{Ca} = 3\cdot10^{-10}\ m^2/s$
Diffusion of CalB (with and without Ca^{2+})	$D_{CalB} = 2\cdot10^{-11}\ m^2/s$
Diffusion of indicator*	$D_{Indo} = 10^{-26}\ m^2/s$

* - as the simulation programme did not allow us to set the diffusion constant of $IndoL_1$ to 0, we chose a number sufficiently low to be negligible.

Theoretical I_{405}/I_{520} profiles were calculated from computational and experimental data via the formula:

$$\frac{I_{405}}{I_{520}} = \frac{C_{Indo} * k_{In405} + C_{CaIndo} * k_{Ca405}}{C_{Indo} * k_{In520} + C_{CaIndo} * k_{Ca520}}$$

Where: C_{Indo} = computed concentration of Ca^{2+}-free fluorophore; C_{CaIndo} = computed concentration of Ca^{2+}-bound fluorophore; k_{In405} = fluorescence intensity for Ca^{2+}-free image with emission filter centered at 405 nm; k_{Ca405} = fluorescence intensity for Ca^{2+}-saturated image with emission filter centered at 405 nm; k_{In520} = fluorescence intensity for Ca^{2+}-free image with emission filter centered at 520 nm; k_{Ca520} = fluorescence intensity for Ca^{2+}-saturated image with emission filter centered at 520 nm. For experiment with CalB: k_{In405} = 2800; k_{In520} = 4100; k_{Ca405} = 3400; k_{Ca520} = 2400.

We can visualize the concentrations of all species involved in the RD experiment at different moments in time (Table S3). We clearly see buffering of Ca^{2+} by CalB, with bands visible for CalB with 1-3 bound Ca^{2+}, and a very broad region close to the contact area with the stamp for fully saturated CalB (four bound Ca^{2+}). This analysis may help to understand the role of CalB and its properties (such as number of binding sites) in localization of Ca^{2+} signals in neurons. Furthermore, we can visualize the amount of Ca^{2+}-bound or -free $IndoL_1$, which are the species that we monitor during the RD experiment.

Table S3: Profiles of intermediate species obtained with our model in COMSOL:

Species	**t = 2 min**	**t = 19 min**
Calbindin·Ca	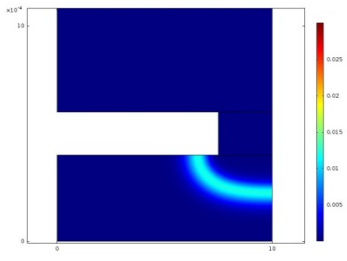	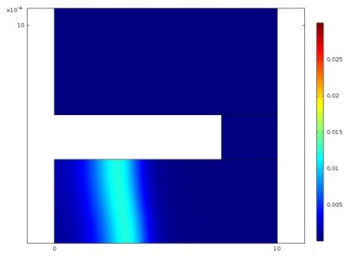

Calbindin·2Ca	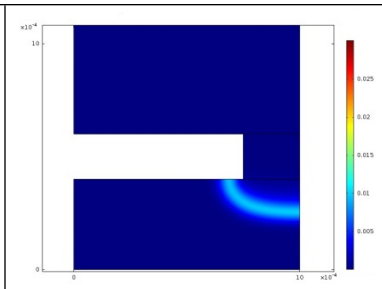	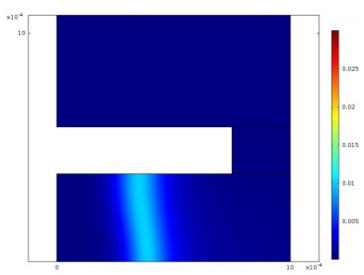
Calbindin·3Ca	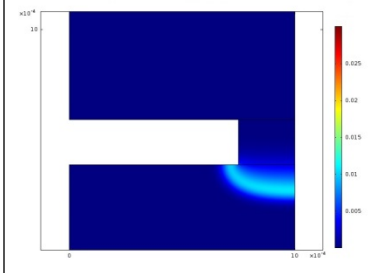	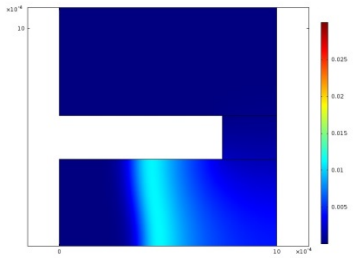
Calbindin·4Ca	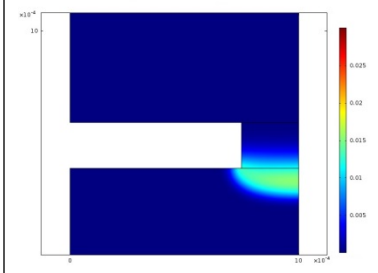	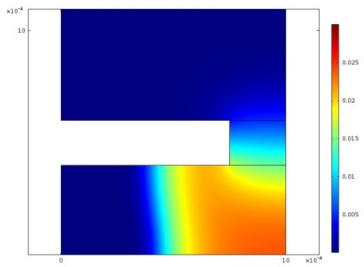
Indo-1·Ca	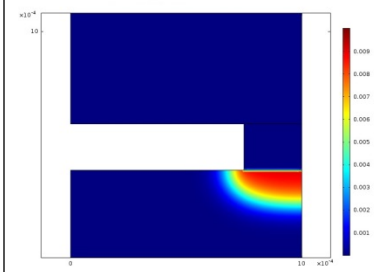	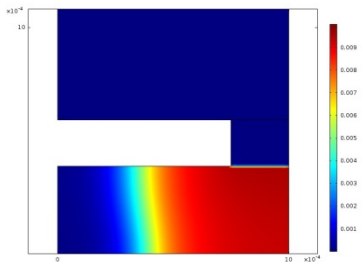

10. References

1. R. M. Sánchez-Martín, M. Cuttle, S. Mittoo, and M. Bradley, *Angew. Chem. Int. Ed. Engl.*, 2006, **45**, 5472–5474.

2. M. Bannwarth, I. R. Correa, M. Sztretye, S. Pouvreau, C. Fellay, A. Aebischer, L. Royer, E. Rois, and K. Johnsson, *ACS Chem. Biol.*, 2009, **4**, 179–190.

3. H. Yu, Z. Feng, A. Zhang, L. Sun, and L. Qian, *Soft Matter*, 2006, **2**, 343–349.

4. Y. Wei, P. J. Wesson, I. Kourkine, and B. A. Grzybowski, *Anal. Chem.*, 2010, **82**, 8780–8784.

5. S. N. Semenov, A. J. Markvoort, W. B. L. Gevers, A. Piruska, T. F. A. de Greef, and W. T. S. Huck, *Biophys. J.*, 2013, **105**, 1057–1066.

6. T. Berggård, S. Miron, P. Önnerfjord, E. Thulin, K. S. Åkerfeldt, J. J. Enghild, M. Akke, and L. S., *J. Biol. Chem.*, 2002, **277**, 16662–16672.

7. B. Schwaller, M. Meyer, and S. Schiffmann, *Cerebellum*, 2002, **1**, 241–258.

8. B. Y. Z. Zhou and E. Neher, *J. Physiol.*, 1993, **469**, 245–273.